

Thermal and Conductometric Investigations and Phase Diagram of the $\text{Rb}_2\text{S}_2\text{O}_7\text{--V}_2\text{O}_5$ System

F. Abdoun,[†] G. Hatem,[†] M. Gaune-Escard,[†] K. M. Eriksen,[‡] and R. Fehrmann^{*,‡}

Institut Universitaire des Systemes Thermiques Industrielle, Technopole de Chateau-Gombert, rue Enrico Fermi 5, 13453 Marseille, France, and Department of Chemistry, Technical University of Denmark, DK-2800 Lyngby, Denmark

Received: December 2, 1998; In Final Form: March 3, 1999

The catalytically interesting binary system $\text{Rb}_2\text{S}_2\text{O}_7\text{--V}_2\text{O}_5$ has been investigated by means of calorimetric and conductometric methods. Seventeen different compositions of the binary system in the mole fraction range $X_{\text{V}_2\text{O}_5} = 0\text{--}0.45$ have been investigated, and the phase transition temperatures obtained. Based on these, the phase diagram of the $\text{Rb}_2\text{S}_2\text{O}_7\text{--V}_2\text{O}_5$ system has been constructed in the indicated composition range. The phase diagram exhibits a local maximum at $X_{\text{V}_2\text{O}_5} = 0.33$ and probably also at $X_{\text{V}_2\text{O}_5} = 0.5$. This corresponds to the formation of two compounds $\text{Rb}_4(\text{VO})_2\text{O}(\text{SO}_4)_4$ and RbVO_2SO_4 , respectively, as found previously in the analogous Cs system. Two eutectics were found at $X_{\text{V}_2\text{O}_5} = 0.175$ and $X_{\text{V}_2\text{O}_5} = 0.43$, with the temperatures of fusion of 348 °C and 397 °C, respectively. The conductivities of each of the 15 molten mixtures investigated have been expressed by polynomials of the form $\kappa = A(X) + B(X)(t - 470) + C(X)(t - 470)^2 + D(X)(t - 470)^3$. The conductivity of the $\text{Rb}_2\text{S}_2\text{O}_7\text{--V}_2\text{O}_5$ system decreases by increasing mole fraction $X_{\text{V}_2\text{O}_5}$ in the melt, indicating decreasing ionic character of the melt. A comparison is made with the analogous Na, K, and Cs systems.

Introduction

The molten salt/gas system $\text{M}_2\text{S}_2\text{O}_7\text{--V}_2\text{O}_5/\text{SO}_2\text{--O}_2\text{--SO}_3\text{--N}_2$ ($\text{M} = \text{alkali}$) at 400–600 °C is considered^{1,2} a realistic model of the industrial catalyst used for the oxidation of SO_2 to SO_3 and further production of sulfuric acid. Previously, (ref 3 and references therein) we have investigated the deactivation, compound formation, and the complex and redox chemistry of V(V), V(IV), and V(III) in model melts and commercial catalysts. To obtain catalysts with low temperatures of fusion (<350 °C), knowledge of the phase diagrams of the $\text{M}_2\text{S}_2\text{O}_7\text{--V}_2\text{O}_5$ systems may prove useful. Earlier we constructed the phase diagrams of the catalyst model systems $\text{Cs}_2\text{S}_2\text{O}_7\text{--V}_2\text{O}_5$,⁴ $\text{M}_2\text{S}_2\text{O}_7\text{--V}_2\text{O}_5$ ($\text{M} = 80\% \text{ K} + 20\% \text{ Na}$),⁵ $\text{K}_2\text{S}_2\text{O}_7\text{--V}_2\text{O}_5$,⁶ and the catalyst solvent systems under “wet” conditions $\text{K}_2\text{S}_2\text{O}_7\text{--KHSO}_4$ ⁷ and $\text{Na}_2\text{S}_2\text{O}_7\text{--NaHSO}_4$.⁸ Compounds such as $\text{M}_4(\text{VO})_2\text{O}(\text{SO}_4)_4$, MVO_2SO_4 ($\text{M} = \text{K, Cs}$) have been isolated and characterized by X-ray- and spectroscopic methods^{9–12} and in addition a compound with the composition $3\text{K}_2\text{S}_2\text{O}_7\cdot\text{V}_2\text{O}_5$ seems to be formed in the $\text{K}_2\text{S}_2\text{O}_7\text{--V}_2\text{O}_5$ system.⁶ Earlier¹³ investigations of the compound formation in the $\text{Rb}_2\text{S}_2\text{O}_7\text{--V}_2\text{O}_5$ system point to the existence of two compounds with the stoichiometry $2\text{Rb}_2\text{S}_2\text{O}_7\cdot\text{V}_2\text{O}_5$ and $\text{Rb}_2\text{S}_2\text{O}_7\cdot\text{V}_2\text{O}_5$, respectively analogous to what we have found for the Cs system.^{9,12} The present investigation deals with the phase diagram of the $\text{Rb}_2\text{S}_2\text{O}_7\text{--V}_2\text{O}_5$ system, which has not been studied previously.

Experimental Section

Chemicals. The hygroscopic $\text{Rb}_2\text{S}_2\text{O}_7$ is not commercially available nor is $\text{Rb}_2\text{S}_2\text{O}_8$ that can be decomposed to $\text{Rb}_2\text{S}_2\text{O}_7$ at around 300 °C in dry N_2 atmosphere. $\text{Rb}_2\text{S}_2\text{O}_8$ was prepared by mixing solutions of $(\text{NH}_4)_2\text{S}_2\text{O}_8$ and RbOH in water as earlier described⁴ for $\text{Cs}_2\text{S}_2\text{O}_8$. Further thermal conversion to $\text{Rb}_2\text{S}_2\text{O}_7$

and handling of the product were also performed as previously.⁴ The non-hygroscopic V_2O_5 used was from CERAC (99.9%). All handling of chemicals was performed in a drybox with a water content currently checked to be less than around 5 ppm.

Conductivity. The conductivity cell is made of borosilicate glass, where gold electrodes are fused into the bottom of the two compartments containing the melt, in contact via a capillary tube of around 1 mm i.d., as described earlier in detail.¹⁴ The cell was loaded by cutting the stem open in the glovebox and resealing it under around 0.9 atm O_2 (g) to prevent possible reduction of V(V) to V(IV). The cell was mounted in an aluminum block furnace regulated to within ± 0.1 °C. When stable, the conductivity was measured by a Radiometer CDM-230 or CDM-83 conductivity meter. Calibration of the cell was made at room temperature by use of 0.1 demal KCl standard solution as described in the literature.¹⁵ The conductivity of the ionic melt is usually⁶ given by the expression

$$\kappa = A_{\kappa} e^{-E_{\kappa}/RT} \quad (1)$$

where κ is the conductivity, A_{κ} is a constant, and E_{κ} is the activation energy for the migration of the conducting ions. Especially because E_{κ} changes when the phase changes, a marked change of the conductivity is observed at the phase transition temperatures. Thus, from plots of $-\ln(\kappa)$ vs $1/T$ the liquidus and solidus temperatures of the samples might be identified.

Calorimetric Measurements. The thermal measurements of the binary $\text{Rb}_2\text{S}_2\text{O}_7\text{--V}_2\text{O}_5$ system were performed by a Setaram DSC 121 differential scanning calorimeter with change of temperature in steps of 2–5 °C/min. The samples of around 0.5 g were contained in sealed Pyrex cells. The calorimeter was calibrated by fusion of lead and zinc.

Results and Discussion

The conductivity of 14 different compositions of the solid and molten binary $\text{Rb}_2\text{S}_2\text{O}_7\text{--V}_2\text{O}_5$ system has been measured

[†] Technopole de Chateau-Gombert.

[‡] Technical University of Denmark.

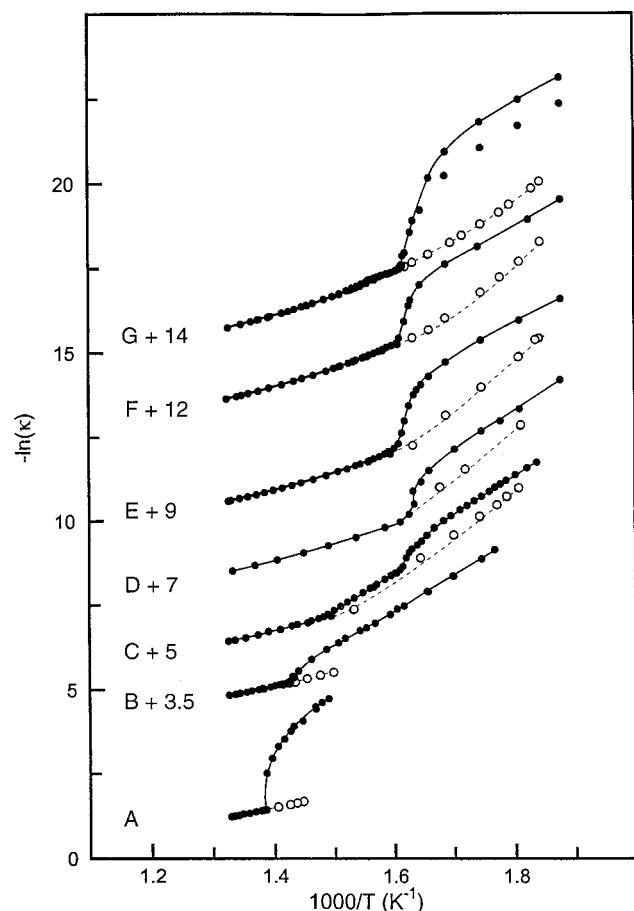


Figure 1. Electrical conductivities in the $\text{Rb}_2\text{S}_2\text{O}_7\text{--V}_2\text{O}_5$ system with $-\ln(\kappa)$ vs $1/T$ for the following compositions $X_{\text{V}_2\text{O}_5}$: A, 0.0000; B, 0.0506; C, 0.1003; D, 0.1377; E, 0.1499; F, 0.1759; G, 0.1980. For clarity the data except those of pure $\text{Rb}_2\text{S}_2\text{O}_7$ are offset on the ordinate by the specified values. Open circles indicate subcooling.

in the temperature range 300–500 °C. The results are shown in Figures 1 and 2. The samples rich in $\text{Rb}_2\text{S}_2\text{O}_7$ crystallized rather easily, but increased tendency to subcooling and glass formation appeared on increase of the V_2O_5 content. Glass formation makes the measurement of phase transition temperatures by conductivity or DSC impossible. In the analogous $\text{K}_2\text{S}_2\text{O}_7\text{--V}_2\text{O}_5$ system⁶ this was a severe problem at high mole fractions of V_2O_5 , while in the present work on the $\text{Rb}_2\text{S}_2\text{O}_7\text{--V}_2\text{O}_5$ system crystallization took place in the subcooled samples after several hours at around 300 °C as was experienced^{4,11} in the $\text{Cs}_2\text{S}_2\text{O}_7\text{--V}_2\text{O}_5$ system as well.

Large jumps of κ to lower values ($-\ln(\kappa)$ to higher) are observed when the subcooled liquid crystallizes. By reheating in small steps, i.e., 2–5 °C, an accurate value of the liquidus temperature is obtained, i.e., where the conductivity returns to the previous value measured during cooling of the initially molten sample. Also, the fusion of the eutectics (the solidus temperature) is observed as breaks in the plots in Figures 1 and 2.

To verify the phase transition temperatures obtained by conductometry, two compositions, i.e., $X_{\text{V}_2\text{O}_5} = 0.182$ and 0.333 were investigated by DSC. All results of the two methods are given in Table 1 and displayed in Figure 3, the $\text{Rb}_2\text{S}_2\text{O}_7\text{--V}_2\text{O}_5$ phase diagram. A good accordance is observed for the results obtained by the two methods. The temperature of fusion of 451 °C found here for $\text{Rb}_2\text{S}_2\text{O}_7$ is in agreement with our previously¹⁶ published value of 450 °C, but far from 401 °C, the only previously¹⁷ published melting point. A maximum is observed

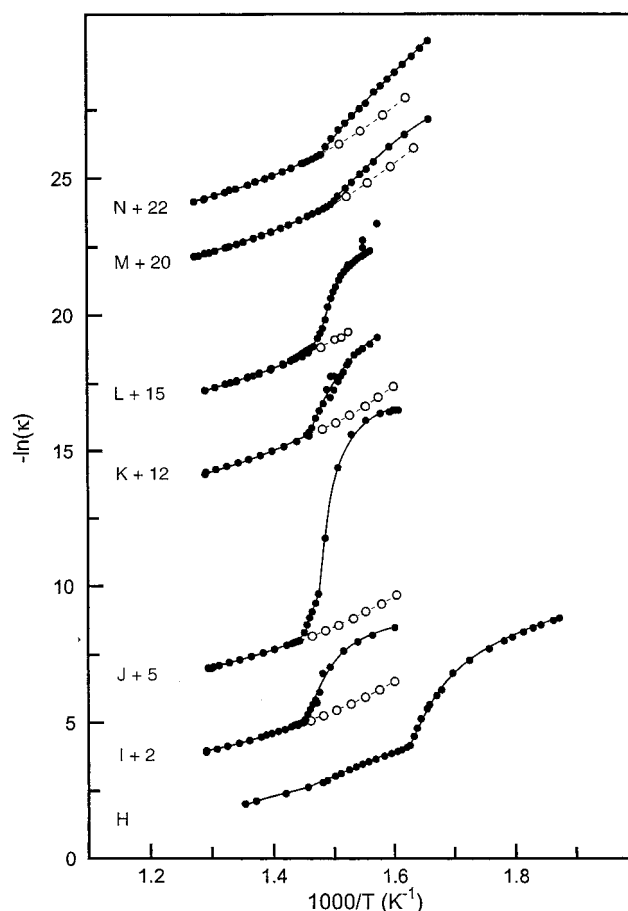


Figure 2. Electrical conductivities in the $\text{Rb}_2\text{S}_2\text{O}_7\text{--V}_2\text{O}_5$ system with $-\ln(\kappa)$ vs $1/T$ for the following compositions $X_{\text{V}_2\text{O}_5}$: H, 0.2505; I, 0.2999; J, 0.3256; K, 0.3915; L, 0.4125; M, 0.4288; N, 0.4499. For clarity, the data (except composition H) are offset on the ordinate by the specified values. Open circles indicate subcooling.

TABLE 1: Conductivity and Differential Thermal Analysis on the $\text{Rb}_2\text{S}_2\text{O}_7\text{--V}_2\text{O}_5$ System: Temperature of Transitions (°C)

$X(\text{V}_2\text{O}_5)$	fusion of eutectic 1		fusion of eutectic 2		liquidus temperature	
	conduct.	DSC	conduct.	DSC	conduct.	DSC
0.0000					451	435 (448 top)
0.0506					431	
0.1003	348				402	
0.1377	348					
0.1499	349				369	
0.1759	350					
0.182		344				364
0.1980	348				370	
0.2505	342				402	
0.2999					417	
0.3256					420	
0.333						414
0.3915					413	
0.4125			399		408	
0.4288			394			
0.4499					402	

in Figure 3 at $X_{\text{V}_2\text{O}_5} = 0.33$ and 414 °C. In the $\text{Cs}_2\text{S}_2\text{O}_7\text{--V}_2\text{O}_5$ phase diagram⁴ a maximum was similarly observed at the same composition. The compound $\text{Cs}_4(\text{VO})_2\text{O}(\text{SO}_4)_4$ having stoichiometry corresponding to this molar ratio was isolated and characterized.⁹ Very recently¹⁸ we have isolated single crystals of V(V) compounds from both the $\text{K}_2\text{S}_2\text{O}_7\text{--V}_2\text{O}_5$ and the $\text{Rb}_2\text{S}_2\text{O}_7\text{--V}_2\text{O}_5$ systems and X-ray investigations reveal a very similar structure as found for $\text{Cs}_4(\text{VO})_2\text{O}(\text{SO}_4)_4$ with separate dimers, $(\text{VO})_2\text{O}(\text{SO}_4)_4^{4-}$, where the VO^{3+} units are joined by

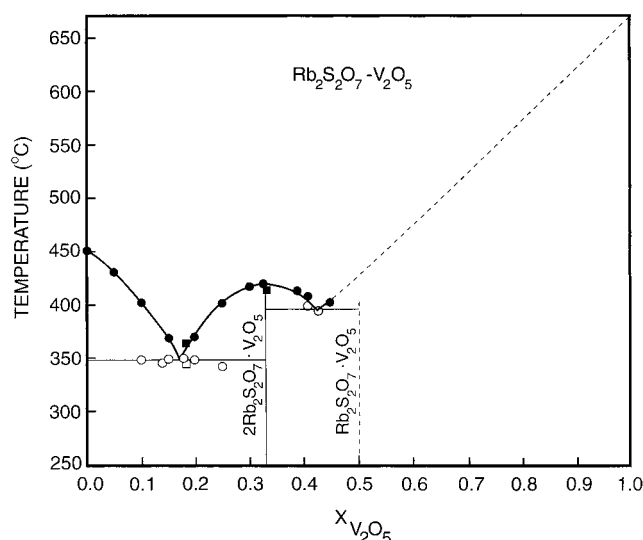


Figure 3. Phase diagram of the $\text{Rb}_2\text{S}_2\text{O}_7\text{--V}_2\text{O}_5$ system obtained from conductivity (●) and DSC (■) measurements. Open symbols indicate the melting temperature of an eutectic phase. The compositions of the possible compounds formed in the system are as indicated. Dashed lines indicate a suggested compound and a suggested liquidus line.

TABLE 2: Compositions and Temperatures (°C) of Fusion of Eutectics and Compounds Formed in the $\text{M}_2\text{S}_2\text{O}_7\text{--V}_2\text{O}_5$ Systems^a

M	eutectic 1		eutectic 2		eutectic 3		compounds			
	X	t	X	t	X	t	X	t	X	t
K	0.174	314	0.27	348	0.39	366	0.25	352	0.33	398
Rb	0.175	348			0.43	397			0.33	414
Cs	0.168	344			0.40	397			0.33	412

^a X = $X_{\text{V}_2\text{O}_5}$.

an oxide bridge and the sulfate ligands are bidentately coordinated, leading to the usual distorted coordination octahedra around V(V). Thus the maximum at $X_{\text{V}_2\text{O}_5} = 0.33$ in the $\text{Rb}_2\text{S}_2\text{O}_7\text{--V}_2\text{O}_5$ phase diagram most probably corresponds to the formation of a compound by the reaction $2\text{Rb}_2\text{S}_2\text{O}_7 + \text{V}_2\text{O}_5 \rightarrow \text{Rb}_4(\text{VO})_2\text{O}(\text{SO}_4)_4$. In the $\text{Cs}_2\text{S}_2\text{O}_7\text{--V}_2\text{O}_5$ system, work in progress¹² shows that the compound CsVO_2SO_4 is formed. It has the molar ratio Cs/V = 1:1 corresponding to the reaction $\text{Cs}_2\text{S}_2\text{O}_7 + \text{V}_2\text{O}_5 \rightarrow 2\text{CsVO}_2\text{SO}_4$. A maximum should be expected in the phase diagram at $X_{\text{V}_2\text{O}_5} = 0.5$, and it is indicated by dashed lines in both the previously⁴ given phase diagram of the $\text{Cs}_2\text{S}_2\text{O}_7\text{--V}_2\text{O}_5$ system and by analogy for the $\text{Rb}_2\text{S}_2\text{O}_7\text{--V}_2\text{O}_5$ phase diagram presented in Figure 3. Above $X_{\text{V}_2\text{O}_5} = 0.5$, the liquidus curve must raise steeply to the temperature of fusion of V_2O_5 of 670 °C. Attempts to investigate the region around $X_{\text{V}_2\text{O}_5} = 0.5$ failed because of experimental difficulties such as high viscosity of the melts, strong tendency to glass formation, softening of the borosilicate glass cell, and decomposition of the melts (to $\text{SO}_3(\text{g})$ and oxides) at elevated temperatures.

The characteristic features of the $\text{Rb}_2\text{S}_2\text{O}_7\text{--V}_2\text{O}_5$ phase diagram are summarized in Table 2 and compared with the previously studied K and Cs analogues. Similar diagrams for the Li and Na analogous systems cannot be obtained because of decomposition of the alkali pyrosulfates. However, the phase diagram for the mixed cation system $\text{M}_2\text{S}_2\text{O}_7\text{--V}_2\text{O}_5$ (M = 0.2 Na + 0.8 K) could be obtained.⁵ It exhibits a maximum at $X_{\text{V}_2\text{O}_5} = 0.25$ and eutectics at 0.175 and 0.30, respectively.

Liquid $\text{Rb}_2\text{S}_2\text{O}_7\text{--V}_2\text{O}_5$ System. As previously^{14,19} for the K and Cs analogous systems, the measured conductivities of the $\text{Rb}_2\text{S}_2\text{O}_7\text{--V}_2\text{O}_5$ system above the liquidus temperatures have

TABLE 3: Coefficients for Empirical Equations^a for the Specific Conductivity of Different Compositions of the Molten $\text{Rb}_2\text{S}_2\text{O}_7\text{--V}_2\text{O}_5$ System

X (V_2O_5)	A(X) ($\Omega^{-1} \text{ cm}^{-1}$)	B(X) ($10^{-3} \Omega^{-1} \text{ cm}^{-1} \text{ deg}^{-1}$)	C(X) ($10^{-6} \Omega^{-1} \text{ cm}^{-1} \text{ deg}^{-2}$)	D(X) ($10^{-8} \Omega^{-1} \text{ cm}^{-1} \text{ deg}^{-3}$)	SD ($\Omega^{-1} \text{ cm}^{-1}$)
0.0000	0.273826	1.6885	1.0269	23.948	0.00197
0.0506	0.247314	1.5587	-4.4610	-6.0330	0.00181
0.1003	0.221815	1.5895	0.12573	-1.3540	0.00250
0.1377	0.208710	1.6893	3.6670	0.29660	0.00054
0.1499	0.189906	1.4128	0.87231	-0.65760	0.00065
0.1759	0.175511	1.4144	1.6427	-0.52350	0.00052
0.1980	0.160772	1.3259	0.62812	-1.1910	0.00097
0.2505	0.142834	1.3992	5.4104	3.2323	0.00081
0.2800	0.122897	1.2481	2.2929	-0.70940	0.00014
0.2999	0.105492	1.1937	1.6541	-1.9550	0.00167
0.3256	0.101001	1.1557	3.0699	0.33835	0.00114
0.3915	0.076246	1.0265	5.1829	3.3047	0.00180
0.4125	0.074038	0.9460	-2.6212	-1.2182	0.00104
0.4288	0.074080	0.9812	2.2142	-1.3370	0.00071
0.4499	0.071537	0.9701	3.3877	-0.01578	0.00090

^a $\kappa = A(X) + B(X)(t - 470) + C(X)(t - 470)^2 + D(X)(t - 470)^3$.

been expressed by polynomials of the type $\kappa = A(X) + B(X)(t - 470) + C(X)(t - 470)^2 + D(X)(t - 470)^3$, where 470 °C is the average temperature of the measurements. The coefficients found from the least-squares fit at each composition $X_{\text{V}_2\text{O}_5}$ measured are given in Table 3 along with the standard deviation. For $X_{\text{V}_2\text{O}_5} = 0.2800$, the data are not shown in Figures 1 or 2, because only conductivities of the liquid region were obtained. The fits are very good, as the SD values at maximum are around 1% of the measured conductivities.

The conductivity at 480 °C for all measured compositions has been calculated applying the polynomials of Table 3. The result is shown in Figure 4, and for comparison similar curves calculated from the K and Cs analogous systems^{6,19} are included together with the extrapolated conductivity⁵ of molten $\text{M}_2\text{S}_2\text{O}_7$ (M = 0.2 Na + 0.8 K). Thus, for the pure molten alkali pyrosulfates the conductivity decreases steadily in the row Na, K, Rb, Cs, i.e., by increased size (and lower mobility) of the alkali cation. Increased addition of V_2O_5 diminishes the difference, indicating that the similar vanadium oxosulfato complexes formed in all systems carry an increasing part of the current compared to the alkali cations. Probably the polymeric V(V) oxosulfato complexes formed^{20,21} like $(\text{VO}_2\text{SO}_4)_n^{n-}$ at high mole fractions $X_{\text{V}_2\text{O}_5}$ transfer the current by a chain mechanism, and at the same time the network structure of the melt reduces the mobility of the alkali ions.

Indeed, large negative deviations of the experimental molar conductivity, Λ_{exptl} , of the melt compared to the one calculated, Λ_{calcd} , from the mole-fraction-weighted average conductivity of the pure components $\text{M}_2\text{S}_2\text{O}_7$ (M = K, Cs) and V_2O_5 have been observed previously.^{14,19} Applying the same procedure also for the present $\text{Rb}_2\text{S}_2\text{O}_7\text{--V}_2\text{O}_5$ system, large deviations, calculated as $((\Lambda_{\text{exptl}} - \Lambda_{\text{calcd}})/\Lambda_{\text{calcd}}) \cdot 100$ (%), are found. The density of the $\text{Rb}_2\text{S}_2\text{O}_7\text{--V}_2\text{O}_5$ system is not known, but assuming the density to be additive (reasonable within few % for the K and Cs systems^{14,19}) with respect to the two components, the molar conductivities could be calculated. The density of $\text{Rb}_2\text{S}_2\text{O}_7$ has recently¹⁶ been measured by us, and the density of V_2O_5 vs temperature was obtained from the literature²² as described previously.^{14,19} The negative deviation increases with increasing mole fraction of V_2O_5 , indicating²³ increased complex formation in the melt.

The values obtained at the highest comparable mole fraction, i.e., $X_{\text{V}_2\text{O}_5} = 0.4$, for the three systems investigated are given for two temperatures in Table 4. In all cases, a large negative

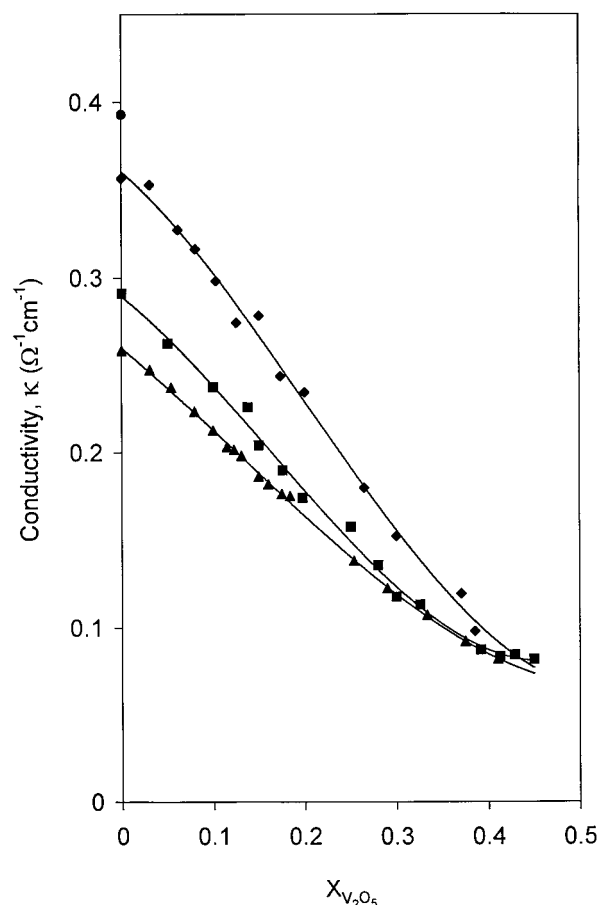


Figure 4. Conductivity isotherms at 480 °C for the molten systems $M_2S_2O_7-V_2O_5$ ($M = 0.2 \text{ Na} + 0.8 \text{ K}$), ● (5); K, ◆ (6); Rb, ■ (this work) and Cs, ▲ (19).

TABLE 4: Comparison of $\left(\frac{\Lambda_{\text{expt}} - \Lambda_{\text{calcd}}}{\Lambda_{\text{calcd}}}\right) 100$ (%) in the $M_2S_2O_7-V_2O_5$ Systems at $X_{V_2O_5} = 0.4$

M	$t = 430$ °C	$t = 480$ °C
K	-58	-34
Rb	-55	-37
Cs	-60	-70

deviation between the experimental and the calculated molar conductivities is observed (highest for the Cs system containing the largest cation), supporting the conclusion given above about the decreased mobility of the alkali cations in the polymeric network of the complexes formed in the melt. Alternatively, different degrees of polymerization for the three systems could also explain the deviations given in Table 4.

Relation to Catalysis. The industrial SO_2 oxidation catalysts are mainly based on K as the promoter, but other alkali ions (i.e., Na and Cs) have also been mixed²⁴ with K in order to enhance the catalytic activity at lower temperatures (i.e., < 440 °C). The present work concludes the series of investigations of the pure binary $M_2S_2O_7-V_2O_5$ systems ($M = \text{K, Rb, or Cs}$) that are possible to study without decomposition of the alkali pyrosulfate. Both of our previously published phase diagrams of the K and Cs systems and the present Rb system (preliminary results in ref 25) show a low melting eutectic around $X_{V_2O_5} = 0.18$, close to the usually applied composition range, $X_{V_2O_5} = 0.20-0.33$, of industrial catalysts. This eutectic represents for each promoter system probably the lower limit of operation

temperature for the liquid oxidized form of the catalyst, assuming that the SO_3 produced is not absorbed to any important extent of the melt. Previously,⁵ we have studied the K system substituted by 20% Na which reflects the composition of the most widespread catalyst in the past. The addition of Na suppresses the freezing point of the melt in the industrial composition range up to about 70 °C, compared to a solely K-promoted catalyst. In recent years also Cs has been added with a positive catalytic effect. If small amounts of Rb also are found to improve the catalyst, it may be used despite that it is several times more expensive than Cs. Systematic investigations by us of the influence of mixed alkali promoter systems including Cs and Rb on the temperature of fusion are in progress. It should, however, be emphasized that the properties of the working industrial catalyst and model systems in contact with $SO_2-O_2-SO_3-N_2$ gas mixtures, i.e., in a partly reducing atmosphere, are most important to study if realistic proposals for the chemistry, reaction mechanism, and optimization of the catalyst are to be put forward.³

Acknowledgment. The Danish Natural Science Research Council and ICAT (Interdisciplinary Center for Catalysis), Technical University of Denmark, have supported this investigation.

References and Notes

- (1) Topsoe, H. F. A.; Nielsen, A. *Trans. Dan. Acad. Tech. Sci.* **1947**, 1, 18.
- (2) Villadsen, J.; Livbjerg, H. *Catal. Rev.-Sci. Eng.* **1978**, 17, 203.
- (3) Lapina, O. B.; Bal'zhinimaev, B. S.; Boghosian, S.; Eriksen, K. M.; Fehrmann, R. *Catal. Today*, in press.
- (4) Folkmann, G. E.; Hatem, G.; Fehrmann, R.; Gaune-Escard, M.; Bjerrum, N. J. *Inorg. Chem.* **1991**, 30, 4057.
- (5) Karydis, D. A.; Boghosian, S.; Fehrmann, R. *J. Catal.* **1994**, 145, 312.
- (6) Folkmann, G. E.; Eriksen, K. M.; Fehrmann, R.; Gaune-Escard, M.; Hatem, G.; Lapina, O. B.; Tersikh, V. *J. Phys. Chem.* **1998**, 102, 24.
- (7) Eriksen, K. M.; Fehrmann, R.; Hatem, G.; Gaune-Escard, M.; Lapina, O. B.; Mastikhin, V. M. *J. Phys. Chem.* **1996**, 100, 10771.
- (8) Hatem, G.; Gaune-Escard, M.; Rasmussen, S. B.; Fehrmann, R. *J. Phys. Chem.* **1999**, 103, 1027-1030.
- (9) Nielsen, K.; Fehrmann, R.; Eriksen, K. M. *Inorg. Chem.* **1993**, 32, 4825.
- (10) Lapina, O. B.; Mastikhin, V. M.; Shubin, A. A.; Eriksen, K. M.; Fehrmann, R. *J. Mol. Catal.* **1995**, 99, 123.
- (11) Lapina, O. B.; Tersikh, V. V.; Shubin, A. A.; Mastikhin, V. M.; Eriksen, K. M.; Fehrmann, R. *J. Phys. Chem.* **1997**, 101, 9188.
- (12) Nielsen, K.; Eriksen, K. M.; Fehrmann, R., in preparation.
- (13) Glazyrin, M. P.; Krasil'nikov, V. N.; Ivakin, A. A. *Russ. J. Inorg. Chem.* **1982**, 27 (12), 1740.
- (14) Hatem, G.; Fehrmann, R.; Gaune-Escard, M.; Bjerrum, N. J. *J. Phys. Chem.* **1987**, 91, 195.
- (15) Jones, G.; Bradshaw, B. C. *J. Am. Chem. Soc.* **1933**, 55, 1780.
- (16) Hatem, G.; Abdoun, F.; Gaune-Escard, M.; Eriksen, K. M.; Fehrmann, R. *Thermochim. Acta* **1998**, 319, 33.
- (17) Spitsyn, V. I.; Meerov, M. A. *Zh. Obshch. Khim.* **1952**, 22, 905.
- (18) Nielsen, K.; Eriksen, K. M.; Fehrmann, R., in preparation.
- (19) Folkmann, G. E.; Hatem, G.; Fehrmann, R.; Gaune-Escard, M.; Bjerrum, N. J. *Inorg. Chem.* **1993**, 32, 1559.
- (20) Fehrmann, R.; Gaune-Escard, M.; Bjerrum, N. J. *Inorg. Chem.* **1986**, 25, 1132.
- (21) Boghosian, S.; Borup, F.; Chrissanthopoulos, A. *Catal. Lett.* **1997**, 48, 145.
- (22) Pantony, D. A.; Vasu, K. I. *J. Inorg. Nucl. Chem.* **1968**, 30, 433.
- (23) Delimarskii, Iu. K.; Markov, B. F., Eds. *Electrochemistry of Fused Salts*, English Ed.; The Sigma Press: Washington, D.C., 1961.
- (24) Boghosian, S.; Fehrmann, R.; Bjerrum, N. J.; Papatheodorou, G. N. *J. Catal.* **1989**, 119, 121.
- (25) Hatem, G.; Gaune-Escard, M.; Fehrmann, R.; Eriksen, K. M. *Proceedings of the Eleventh International Symposium on Molten Salts*; Trulove, P. C. et al., Eds.; The Electrochemical Society: Pennington, N. J., 1998; 98-11, 483-490.